

# Catalysis Science & Technology

Accepted Manuscript



This is an *Accepted Manuscript*, which has been through the Royal Society of Chemistry peer review process and has been accepted for publication.

*Accepted Manuscripts* are published online shortly after acceptance, before technical editing, formatting and proof reading. Using this free service, authors can make their results available to the community, in citable form, before we publish the edited article. We will replace this *Accepted Manuscript* with the edited and formatted *Advance Article* as soon as it is available.

You can find more information about *Accepted Manuscripts* in the [Information for Authors](#).

Please note that technical editing may introduce minor changes to the text and/or graphics, which may alter content. The journal's standard [Terms & Conditions](#) and the [Ethical guidelines](#) still apply. In no event shall the Royal Society of Chemistry be held responsible for any errors or omissions in this *Accepted Manuscript* or any consequences arising from the use of any information it contains.



Journal Name

ARTICLE

## Effect of CeO<sub>2</sub> for a high-efficiency CeO<sub>2</sub>/WO<sub>3</sub>-TiO<sub>2</sub> catalyst on the N<sub>2</sub>O formation in NH<sub>3</sub>-SCR: a kinetic study

Yang Geng,<sup>a</sup> Wenpo Shan,<sup>a\*</sup> Shangchao Xiong,<sup>a</sup> Yong Liao,<sup>a</sup> Shijian Yang<sup>a</sup> and Fudong Liu<sup>b</sup>

Received 00th January 20xx,  
Accepted 00th January 20xx

DOI: 10.1039/x0xx00000x

www.rsc.org/

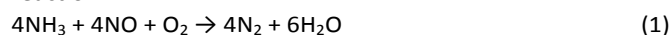
In this study, we investigated the effects of CeO<sub>2</sub> for a high-efficiency CeO<sub>2</sub>/WO<sub>3</sub>-TiO<sub>2</sub> catalyst on the N<sub>2</sub>O formation in NH<sub>3</sub>-SCR reaction using kinetic method. The results demonstrated that CeO<sub>2</sub> is very effective for enhancing SCR (4NH<sub>3</sub> + 4NO + O<sub>2</sub> → 4N<sub>2</sub> + 6H<sub>2</sub>O) reaction rate and thus depressing the NSCR reaction (4NH<sub>3</sub> + 4NO + 3O<sub>2</sub> → 4N<sub>2</sub>O + 6H<sub>2</sub>O) due to the competition between these two reactions. Therefore, the N<sub>2</sub>O formation under SCR reaction condition could be remarkably inhibited with the addition of CeO<sub>2</sub> to the catalyst. On the other hand, CeO<sub>2</sub> can also enhance the C-O reaction (4NH<sub>3</sub> + 5O<sub>2</sub> → 4NO + 6H<sub>2</sub>O) over the catalyst, so the N<sub>2</sub>O formation under NH<sub>3</sub> oxidation condition was promoted due to the lack of SCR reaction. In addition, we also found another interesting phenomenon that the N<sub>2</sub>O formation over WO<sub>3</sub>-TiO<sub>2</sub> (without CeO<sub>2</sub>) decreased gradually at high temperature from 350 to 450 °C, while the N<sub>2</sub>O formation over CeO<sub>2</sub>/WO<sub>3</sub>-TiO<sub>2</sub> kept increasing with the reaction temperature, which was also associated with the promotional effect of CeO<sub>2</sub> on SCR reaction and the competition between SCR and NSCR reactions.

### 1. Introduction

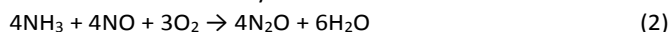
Selective catalytic reduction of NO<sub>x</sub> with NH<sub>3</sub> (NH<sub>3</sub>-SCR) has been widely applied for the removal of NO<sub>x</sub> generated from stationary sources since 1970s.<sup>1</sup> This technology has also become the dominant technology for meeting the ever tightened emission standards.<sup>2,3</sup> Due to the limited space onboard, one of the main challenges for diesel vehicles under increasingly stringent emission legislations is the reduction of catalyst volume, which requires the SCR catalyst should work efficiently under high space velocity conditions.<sup>4</sup>

Great efforts have recently been focused on the optimization of SCR catalysts for enhancing the catalytic efficiency and broadening the temperature window.<sup>2,5,6</sup> Ceria has been shown to be a very effective promoter for MnO<sub>x</sub>-TiO<sub>2</sub>,<sup>7,8</sup> V<sub>2</sub>O<sub>5</sub>/TiO<sub>2</sub>,<sup>9</sup> and Fe-ZSM-5 catalysts<sup>10</sup>. In addition, ceria was widely used as the main active component<sup>11-17</sup> for NH<sub>3</sub>-SCR catalysts.<sup>18</sup> In our previous study, a high-efficient CeO<sub>2</sub>/WO<sub>3</sub>-TiO<sub>2</sub> catalyst was prepared by a novel stepwise precipitation approach.<sup>19</sup> This catalyst showed excellent catalytic performance, with superior SCR activity, high N<sub>2</sub> selectivity and broad operation temperature window, even under extremely high space velocity conditions.

The main reaction under NH<sub>3</sub>-SCR condition is the standard SCR reaction:



At high temperature region, non-selective catalytic reduction reaction (NSCR reaction, reaction 2) and catalytic oxidation of NH<sub>3</sub> (C-O reaction, reaction 3), as two side reactions, will occurred simultaneously:



The formed N<sub>2</sub>O from reaction (2) is a strong greenhouse gas, which is usually notable at high temperatures and is mainly related to the NSCR reaction.<sup>20</sup> Isotopic labelling study has demonstrated that the two N atoms in N<sub>2</sub>O are mainly due to a coupling of one nitrogen atom from NH<sub>3</sub> and the other one from NO.<sup>21</sup>

During the development of the CeO<sub>2</sub>/WO<sub>3</sub>-TiO<sub>2</sub> catalyst, we found that CeO<sub>2</sub> plays a key role in the catalyst for the excellent N<sub>2</sub> selectivity. In this study, we furtherly investigated the effects of CeO<sub>2</sub> for a CeO<sub>2</sub>/WO<sub>3</sub>-TiO<sub>2</sub> catalyst on the N<sub>2</sub>O formation in NH<sub>3</sub>-SCR reaction using kinetic method. Interestingly, we found that CeO<sub>2</sub> was effective for the inhibition of N<sub>2</sub>O formation under SCR reaction condition over the catalyst, while it enhanced the N<sub>2</sub>O formation under NH<sub>3</sub> oxidation condition. In addition, there was a peak of the N<sub>2</sub>O formation at 350 °C over WO<sub>3</sub>-TiO<sub>2</sub>, but when CeO<sub>2</sub> was introduced the N<sub>2</sub>O formation increased continuously with the increase of the reaction temperature over CeO<sub>2</sub>/WO<sub>3</sub>-TiO<sub>2</sub>.

### 2. Experimental

#### 2.1 Catalyst synthesis

The CeO<sub>2</sub>/WO<sub>3</sub>-TiO<sub>2</sub> catalyst was prepared by an optimized precipitation method. Ce(NO<sub>3</sub>)<sub>3</sub>·6H<sub>2</sub>O, (NH<sub>4</sub>)<sub>10</sub>W<sub>12</sub>O<sub>41</sub> and Ti(SO<sub>4</sub>)<sub>2</sub> were dissolved into distilled water together, with a Ce/W/Ti molar ratio of 0.2 : 0.1 : 1.0. Excessive urea was added into the mixed solution and then heated to 90 °C. After vigorous

<sup>a</sup> School of Environmental and Biological Engineering, Nanjing University of Science and Technology, Nanjing 210094, PR China. E-mail: wenposhan@hotmail.com; Fax: +86 25 84315173; Tel: +86 18012920637.

<sup>b</sup> Materials Sciences Division, Lawrence Berkeley National Laboratory, Berkeley 94720, California, United States.

stirring for 12 h, the precipitated solids were collected by filtration and then washed with distilled water, dried at 100 °C for 12 h and calcinated at 500 °C for 5 h, orderly. In addition, a  $\text{WO}_3\text{-TiO}_2$  catalyst was also prepared using the same method as a reference sample.

## 2.2 Catalytic test

Before  $\text{NH}_3\text{-SCR}$  activity test, the powder samples were pressed, crushed and sieved to 40-60 mesh. The SCR activity tests of the sieved powder catalysts were carried out in a fixed-bed quartz flow reactor at atmospheric pressure. The reaction conditions were controlled as follows: 500 ppm  $\text{NO}$ , 500 ppm  $\text{NH}_3$ , 5 vol.%  $\text{O}_2$ ,  $\text{N}_2$  balance, and 400 mL/min total flow rate. The effluent gas, including  $\text{NO}$ ,  $\text{NH}_3$ ,  $\text{NO}_2$  and  $\text{N}_2\text{O}$ , was continuously analyzed by an online FTIR gas analyzer (Nicolet Antaris IGS analyzer). The concentration data were collected after 0.5 h when the SCR reaction reached a steady state.

## 2.3 Reaction kinetic study

To obtain the reaction rate constants of  $\text{N}_2$  and  $\text{N}_2\text{O}$  formation over  $\text{WO}_3\text{-TiO}_2$  and  $\text{CeO}_2/\text{WO}_3\text{-TiO}_2$ , steady-state kinetic investigations were performed. Gaseous  $\text{NH}_3$  concentration in the inlet was kept at 500 ppm, while gaseous  $\text{NO}$  concentration varied from 0 to 700 ppm. To overcome the diffusion limitation (including inner diffusion and external diffusion), very high GHSVs were adopted to obtain less than 20% of  $\text{NO}_x$  conversion. The catalyst mass ranged from 3 to 200 mg for  $\text{WO}_3\text{-TiO}_2$  and from 3 to 4 mg for  $\text{CeO}_2/\text{WO}_3\text{-TiO}_2$ , and the total flow rate was 200 or 400  $\text{mL min}^{-1}$ .

## 2.4 Transient reaction study

To investigate the elemental reaction of  $\text{N}_2\text{O}$  formation over  $\text{WO}_3\text{-TiO}_2$  and  $\text{CeO}_2/\text{WO}_3\text{-TiO}_2$ , transient reaction study was performed. The concentrations of  $\text{NO}$ ,  $\text{NH}_3$ ,  $\text{NO}_2$ , and  $\text{N}_2\text{O}$  in the outlet were recorded during passing 500 ppm of  $\text{NO}$  and 5% of  $\text{O}_2$  over  $\text{NH}_3$  (500 ppm) presorbed catalysts, and passing 500 ppm of  $\text{NH}_3$  over  $\text{NO}$  (500 ppm) +  $\text{O}_2$  (5%) presorbed catalysts, respectively.

## 2.5 In situ DRIFTS

To examine the surface  $\text{NH}_3$  adsorbed species on  $\text{WO}_3\text{-TiO}_2$  and  $\text{CeO}_2/\text{WO}_3\text{-TiO}_2$ , *in situ* DRIFTS study was performed. The *in situ* DRIFTS experiments were carried out on an FTIR spectrometer (Thermo Scientific Nicolet IS50) equipped with a smart collector and a MCT detector cooled by liquid nitrogen. The spectra were collected after the treatment of samples with 500 ppm  $\text{NH}_3$  for 30 min and  $\text{N}_2$  purge for 30 min. All spectra were recorded by accumulating 100 scans with a resolution of 4  $\text{cm}^{-1}$ .

## 3. Results and discussion

### 3.1 $\text{NH}_3\text{-SCR}$ performance

The  $\text{NH}_3\text{-SCR}$  performance of  $\text{WO}_3\text{-TiO}_2$  and  $\text{CeO}_2/\text{WO}_3\text{-TiO}_2$  were tested under a high GHSV of 400,000  $\text{h}^{-1}$  (Fig. 1). The  $\text{WO}_3\text{-TiO}_2$  showed almost no SCR activity in low temperature range. The  $\text{NO}_x$  conversion over  $\text{WO}_3\text{-TiO}_2$  kept increasing with the reaction temperature and reached high level in the high temperature region. With the introduction of  $\text{CeO}_2$  onto the surface of  $\text{WO}_3\text{-TiO}_2$ , the profile of  $\text{NO}_x$  conversion over  $\text{CeO}_2/\text{WO}_3\text{-TiO}_2$  was quite different with that over  $\text{WO}_3\text{-TiO}_2$ . The low-temperature activity over  $\text{CeO}_2/\text{WO}_3\text{-TiO}_2$  was

remarkably enhanced, while the  $\text{NO}_x$  conversion exhibited a decrease trend in high temperature region due to the oxidation of  $\text{NH}_3$ , which even made the  $\text{NO}_x$  conversion over  $\text{CeO}_2/\text{WO}_3\text{-TiO}_2$  being lower than that over  $\text{WO}_3\text{-TiO}_2$  at 450 °C.

The  $\text{N}_2\text{O}$  formation profiles over  $\text{WO}_3\text{-TiO}_2$  and  $\text{CeO}_2/\text{WO}_3\text{-TiO}_2$  were also quite different with each other. The addition of  $\text{CeO}_2$  remarkably inhibited the formation of  $\text{N}_2\text{O}$  during  $\text{NH}_3\text{-SCR}$  reaction in the whole temperature range. Interestingly, there was a peak value (37.4 ppm) of the  $\text{N}_2\text{O}$  formation appeared at 350 °C over  $\text{WO}_3\text{-TiO}_2$ , while the  $\text{N}_2\text{O}$  formation increased continuously with the increase of the reaction temperature over  $\text{CeO}_2/\text{WO}_3\text{-TiO}_2$ .

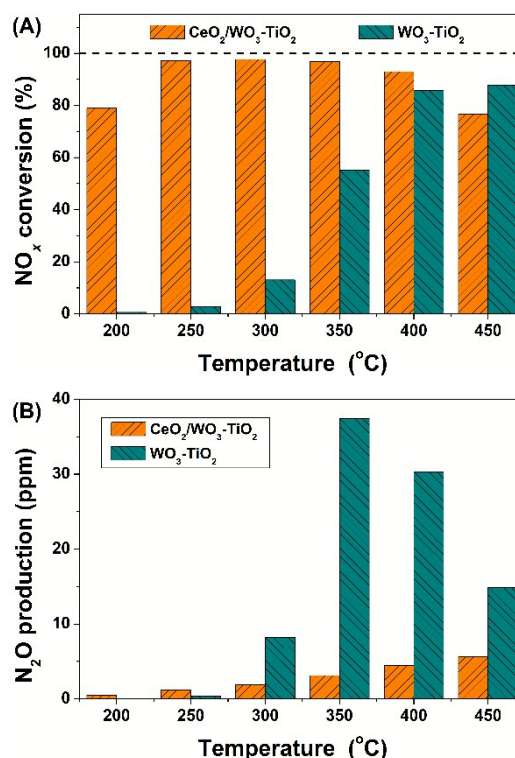


Fig. 1 (A)  $\text{NO}_x$  conversions and (B)  $\text{N}_2\text{O}$  formations during  $\text{NH}_3\text{-SCR}$  reactions over  $\text{WO}_3\text{-TiO}_2$  and  $\text{CeO}_2/\text{WO}_3\text{-TiO}_2$ . Reaction conditions:  $[\text{NO}] = [\text{NH}_3] = 500$  ppm,  $[\text{O}_2] = 5$  vol.%,  $\text{N}_2$  balance and GHSV = 400,000  $\text{h}^{-1}$ .

### 3.2 $\text{NH}_3$ oxidation

To investigate the origination of  $\text{N}_2\text{O}$  over the catalysts,  $\text{NH}_3$  oxidation tests were carried out over  $\text{WO}_3\text{-TiO}_2$  and  $\text{CeO}_2/\text{WO}_3\text{-TiO}_2$  (Fig. 2). The  $\text{NH}_3$  conversion over  $\text{CeO}_2/\text{WO}_3\text{-TiO}_2$  was obviously higher than that over  $\text{WO}_3\text{-TiO}_2$ , indicating that the introduction of  $\text{CeO}_2$  could promote the catalytic oxidation of  $\text{NH}_3$ . Different with the results of  $\text{NH}_3\text{-SCR}$  tests, the  $\text{N}_2\text{O}$  formation profiles over  $\text{WO}_3\text{-TiO}_2$  and  $\text{CeO}_2/\text{WO}_3\text{-TiO}_2$  were similar with each other. Both showed an increase trend of  $\text{N}_2\text{O}$  formation with the increase of reaction temperature. The introduction of  $\text{CeO}_2$  significantly promoted the formation of  $\text{N}_2\text{O}$  during  $\text{NH}_3$  oxidation reaction in the whole temperature range. In addition to  $\text{N}_2\text{O}$ ,  $\text{NO}$  was also detected at high temperature region over both of the catalysts (inserted). The  $\text{NO}$  formation over  $\text{CeO}_2/\text{WO}_3\text{-TiO}_2$  was higher than that over

WO<sub>3</sub>-TiO<sub>2</sub>, and both of them showed an increase trend with the increase of reaction temperature.

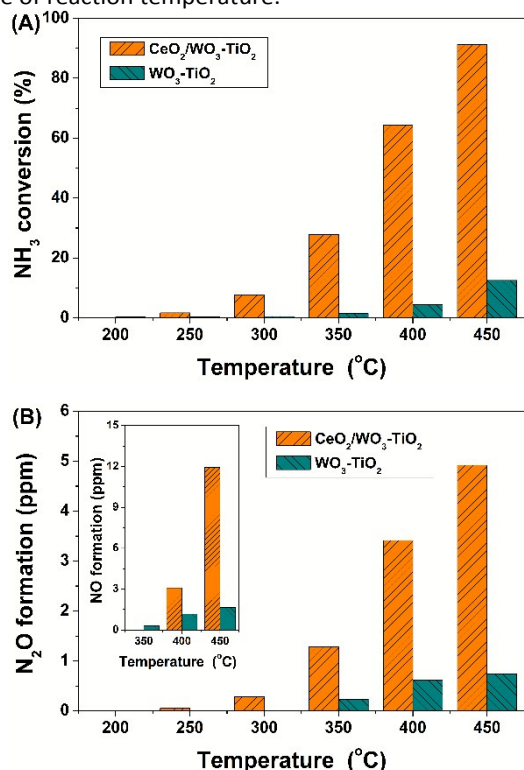


Fig. 2 (A) NH<sub>3</sub> conversions and (B) N<sub>2</sub>O formations during NH<sub>3</sub> oxidation reactions over WO<sub>3</sub>-TiO and CeO<sub>2</sub>/WO<sub>3</sub>-TiO<sub>2</sub>. Reaction conditions: [NH<sub>3</sub>] = 500 ppm, [O<sub>2</sub>] = 5 vol.%, N<sub>2</sub> balance and GHSV = 400,000 h<sup>-1</sup>.

### 3.3 Transient reaction

To investigate the mechanism of N<sub>2</sub>O formation over WO<sub>3</sub>-TiO<sub>2</sub> and CeO<sub>2</sub>/WO<sub>3</sub>-TiO<sub>2</sub>, transient reaction analyses were performed at 350 °C (Fig. 3). When NO + O<sub>2</sub> passed over the NH<sub>3</sub> presorbed catalysts, N<sub>2</sub>O rapidly formed over WO<sub>3</sub>-TiO<sub>2</sub> (Fig. 3A). There was also a small amount of N<sub>2</sub>O formed over CeO<sub>2</sub>/WO<sub>3</sub>-TiO<sub>2</sub> (Fig. 3B). The formation of N<sub>2</sub>O during the tests were mainly through Eley-Rideal mechanism, i.e., the reaction between adsorbed NH<sub>3</sub> species and gaseous NO.<sup>20, 22-24</sup>

On the other hand, when NH<sub>3</sub> passed over NO + O<sub>2</sub> presorbed catalysts, no N<sub>2</sub>O was detected over WO<sub>3</sub>-TiO<sub>2</sub> (Fig. 3C). Small amount of N<sub>2</sub>O with stable concentration was slowly and continuously formed over CeO<sub>2</sub>/WO<sub>3</sub>-TiO<sub>2</sub>, which should be resulted from the NH<sub>3</sub> oxidation (Fig. 3D). It indicates that the N<sub>2</sub>O formation according to Langmuir-Hinshelwood mechanism (the reaction between adsorbed NO<sub>x</sub> and NH<sub>3</sub> species) could be neglected, and the reaction route for N<sub>2</sub>O formation mainly follows Eley-Rideal mechanism under NH<sub>3</sub>-SCR condition over both of the WO<sub>3</sub>-TiO<sub>2</sub> and CeO<sub>2</sub>/WO<sub>3</sub>-TiO<sub>2</sub>.<sup>20, 22-24</sup>

### 3.4 In situ DRIFTS study

The *in situ* DRIFTS of NH<sub>3</sub> adsorption were measured to examine the surface adsorbed NH<sub>3</sub> species on WO<sub>3</sub>-TiO<sub>2</sub> and CeO<sub>2</sub>/WO<sub>3</sub>-TiO<sub>2</sub> (Fig. 4). After NH<sub>3</sub> adsorption at 350 °C, the observed bands at 1605 cm<sup>-1</sup> and 1256, 1226/1249, 1220 cm<sup>-1</sup> can be assigned to the asymmetric and symmetric bending vibrations of coordinated NH<sub>3</sub> linked to Lewis acid sites;<sup>25-27</sup> the bands at 3260, 3352 and 3385 cm<sup>-1</sup> are assigned to the N-H stretching

vibration modes of the coordinated NH<sub>3</sub>;<sup>26,28</sup> the bands at 1422 cm<sup>-1</sup> are assigned to the symmetric and asymmetric bending vibrations of NH<sub>4</sub><sup>+</sup> on Brønsted acid sites,<sup>28-30</sup> and the bands at 3685 and 3645 cm<sup>-1</sup> are assigned to the hydroxyl consumption due to the interaction with NH<sub>3</sub> to form NH<sub>4</sub><sup>+</sup>.<sup>25,28</sup> When the reaction temperature was decreased to 250 °C, a band at 1553 cm<sup>-1</sup> due to the scissoring vibration mode of NH<sub>2</sub> species was observed on CeO<sub>2</sub>/WO<sub>3</sub>-TiO<sub>2</sub>.<sup>26,31</sup> Since W and Ti species can play as acid sites for NH<sub>3</sub> adsorption, the NH<sub>3</sub> adsorption peaks on WO<sub>3</sub>-TiO<sub>2</sub> were generally higher than those on CeO<sub>2</sub>/WO<sub>3</sub>-TiO<sub>2</sub>. However, the activation of the adsorbed NH<sub>3</sub> species on WO<sub>3</sub>-TiO<sub>2</sub> was much weaker than that on CeO<sub>2</sub>/WO<sub>3</sub>-TiO<sub>2</sub>. Therefore, the band (1553 cm<sup>-1</sup>) associated with NH<sub>2</sub> species was only observed on CeO<sub>2</sub>/WO<sub>3</sub>-TiO<sub>2</sub>. Due to the higher capability for NH<sub>3</sub> activation, CeO<sub>2</sub>/WO<sub>3</sub>-TiO<sub>2</sub> catalyst is more active than WO<sub>3</sub>-TiO<sub>2</sub> for NH<sub>3</sub>-SCR and NH<sub>3</sub> oxidation.

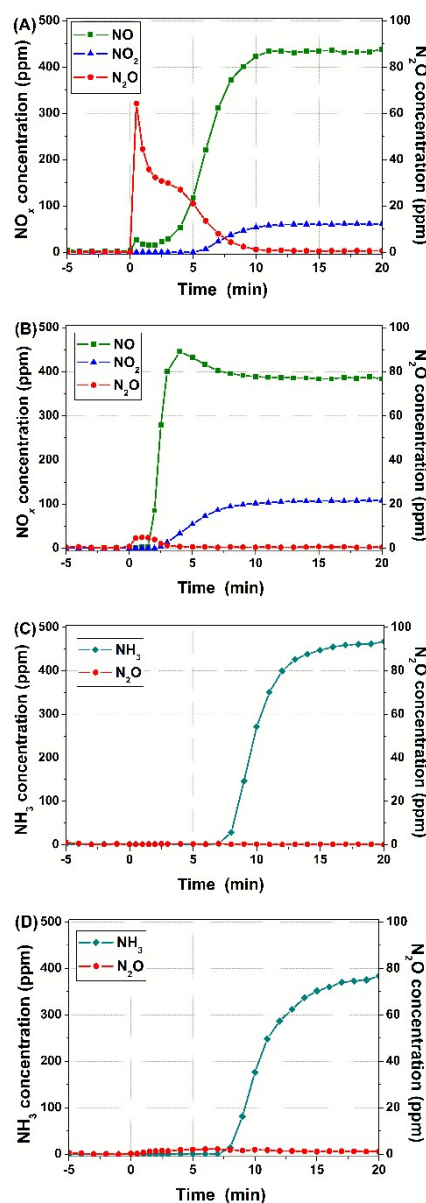
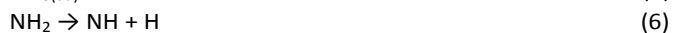


Fig. 3 Transient reactions at 350 °C upon passing 500 ppm NO + 5% O<sub>2</sub> over NH<sub>3</sub> presorbed (A) WO<sub>3</sub>-TiO<sub>2</sub> and (B) CeO<sub>2</sub>/WO<sub>3</sub>-TiO<sub>2</sub> and passing 500 ppm NH<sub>3</sub> over NO + O<sub>2</sub> presorbed (C) WO<sub>3</sub>-TiO<sub>2</sub> and (D) CeO<sub>2</sub>/WO<sub>3</sub>-TiO<sub>2</sub>.

Many previous studies have focused on the reaction mechanisms of NH<sub>3</sub>-SCR and selective catalytic oxidation of NH<sub>3</sub>.<sup>22-24,32</sup> Based on these previous results and the *in situ* DRIFTS, the main reaction routes through Eley-Rideal mechanism can be described as follows:



NH<sub>3</sub> is firstly adsorbed on the surface of catalyst (reaction 4). The adsorbed NH<sub>3</sub> species can be activated to form NH<sub>2</sub> species (reaction 5), and the formed NH<sub>2</sub> can be oxidized to NH (reaction 6). Further oxidation of NH will induce the formation of NO (C-O reaction, reaction 7). On the other hand, the formed NH<sub>2</sub> and NH species on the catalyst surface can react with gaseous NO to form N<sub>2</sub> (SCR reaction, reaction 8) and N<sub>2</sub>O (NSCR reaction, reaction 9), respectively.

All of these three reactions would contribute to NH<sub>3</sub> consumption.<sup>33,34</sup> Therefore, the rate of NH<sub>3</sub> conversion ( $\delta_{\text{NH}_3}$ ) can be described as:

$$\delta_{\text{NH}_3} = \delta_{\text{SCR}} + \delta_{\text{NSCR}} + \delta_{\text{C-O}} \quad (10)$$

Where  $\delta_{\text{SCR}}$ ,  $\delta_{\text{NSCR}}$  and  $\delta_{\text{C-O}}$  refer to the reaction rates of SCR (*i.e.* N<sub>2</sub> formation), NSCR (*i.e.* N<sub>2</sub>O formation), and C-O reactions, respectively.

Both of the SCR and NSCR reactions could contribute to NO consumption, while the C-O reaction contributes to NO formation. Therefore, the rate of NO conversion ( $\delta_{\text{NO}}$ ) can be described as:

$$\delta_{\text{NO}} = \delta_{\text{SCR}} + \delta_{\text{NSCR}} - \delta_{\text{C-O}} \quad (11)$$

From the equations (10) and (11), we can obtain the rate of C-O reaction as:

$$\delta_{\text{C-O}} = (\delta_{\text{NH}_3} - \delta_{\text{NO}})/2 \quad (12)$$

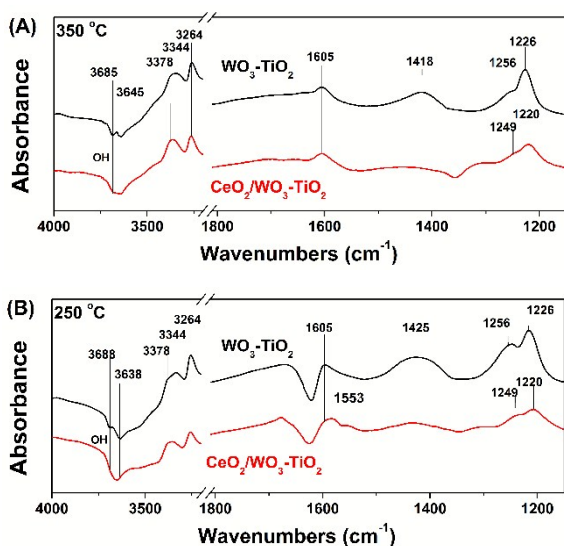


Fig. 4 *In situ* DRIFTS of NH<sub>3</sub> adsorption at (A) 350 °C and (B) 250 °C.

### 3.5 Steady-state reaction kinetic study

**3.5.1 SCR reaction rates** The SCR reaction rate was represented by the N<sub>2</sub> formation rate, while the N<sub>2</sub> formation was calculated by the following equation:

$$\text{N}_2 \text{ formation} = \frac{([\text{NO}_x]_{\text{in}} + [\text{NH}_3]_{\text{in}} - [\text{NO}_x]_{\text{out}} - [\text{NH}_3]_{\text{out}} - 2[\text{N}_2\text{O}]_{\text{out}})/2}{\quad} \quad (13)$$

The SCR reaction rates as a function of NO concentration over WO<sub>3</sub>-TiO<sub>2</sub> and CeO<sub>2</sub>/WO<sub>3</sub>-TiO<sub>2</sub> were shown in Fig. 5. With the increase of NO concentration, both of the reaction rates over WO<sub>3</sub>-TiO<sub>2</sub> and CeO<sub>2</sub>/WO<sub>3</sub>-TiO<sub>2</sub> increased gradually. Furthermore, the SCR reaction rates all showed excellent liner correlation with NO concentrations at each temperature, with the correlation coefficients for WO<sub>3</sub>-TiO<sub>2</sub> and CeO<sub>2</sub>/WO<sub>3</sub>-TiO<sub>2</sub> all over 0.991 and 0.996, respectively. It is consistent with the previous test results on MnO<sub>x</sub>-based catalysts, indicating that the reaction order of SCR over WO<sub>3</sub>-TiO<sub>2</sub> and CeO<sub>2</sub>/WO<sub>3</sub>-TiO<sub>2</sub> with respect to gaseous NO concentration were both nearly 1.<sup>20,24</sup>

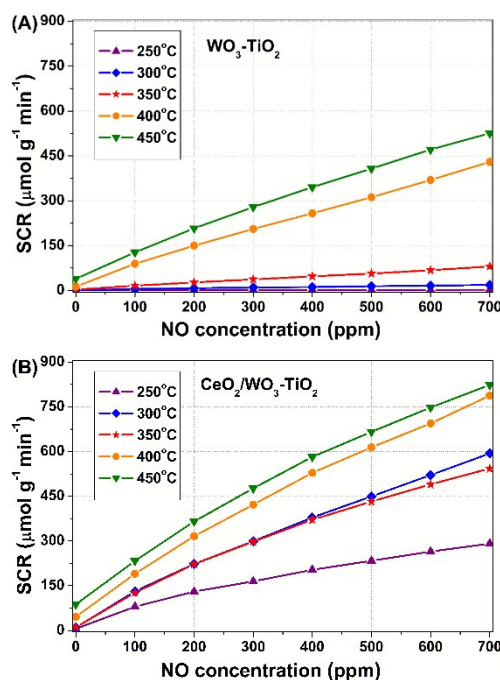


Fig. 5 SCR reaction rates as a function of gaseous NO concentration over (A) WO<sub>3</sub>-TiO<sub>2</sub> and (B) CeO<sub>2</sub>/WO<sub>3</sub>-TiO<sub>2</sub>. Reaction conditions: [NO] = 0-700 ppm, [NH<sub>3</sub>] = 500 ppm, [O<sub>2</sub>] = 5 vol.%, N<sub>2</sub> balance and catalyst mass = 3-200 mg.

At all the tested temperature points from 250 to 450 °C, the SCR reaction rates over CeO<sub>2</sub>/WO<sub>3</sub>-TiO<sub>2</sub> were obviously higher than those over WO<sub>3</sub>-TiO<sub>2</sub>, which is consistent with the SCR activity test result in Fig. 1(A), *i.e.*, the SCR activity of CeO<sub>2</sub>/WO<sub>3</sub>-TiO<sub>2</sub> was much higher than that of WO<sub>3</sub>-TiO<sub>2</sub>.

**3.5.2 C-O reaction rates** The C-O reaction (oxidation of NH<sub>3</sub> to NO) rates, calculated by equation (12), as a function of NO concentration over WO<sub>3</sub>-TiO<sub>2</sub> and CeO<sub>2</sub>/WO<sub>3</sub>-TiO<sub>2</sub> were shown in Fig. 6. Below 350 °C, both of the reaction rates over WO<sub>3</sub>-TiO<sub>2</sub> and CeO<sub>2</sub>/WO<sub>3</sub>-TiO<sub>2</sub> were relatively low. When reaction temperature increased to 400 and 450 °C, the C-O reaction rates were remarkably promoted, particularly for CeO<sub>2</sub>/WO<sub>3</sub>-TiO<sub>2</sub>. It indicates that more NH<sub>3</sub> could be oxidized to NO over

CeO<sub>2</sub>/WO<sub>3</sub>-TiO<sub>2</sub> at high temperature and the C-O reaction would induce significant influence on SCR reaction, which was the reason for the decrease of NO<sub>x</sub> conversions over CeO<sub>2</sub>/WO<sub>3</sub>-TiO<sub>2</sub> during SCR activity test at high temperature, as shown in Fig. 1(A).

From Fig. 6 we can also see that, the C-O reaction rates over WO<sub>3</sub>-TiO<sub>2</sub> and CeO<sub>2</sub>/WO<sub>3</sub>-TiO<sub>2</sub> both decreased with the increase of NO concentration, indicating that the C-O reaction rates over the two catalysts with respect to NO concentration were both lower than 0. At high temperatures, the C-O reaction rates of CeO<sub>2</sub>/WO<sub>3</sub>-TiO<sub>2</sub> were much higher than those of WO<sub>3</sub>-TiO<sub>2</sub>, which is consistent with the NH<sub>3</sub> oxidation results in Fig. 2, with higher NO formation over CeO<sub>2</sub>/WO<sub>3</sub>-TiO<sub>2</sub> at 400 and 450 °C.

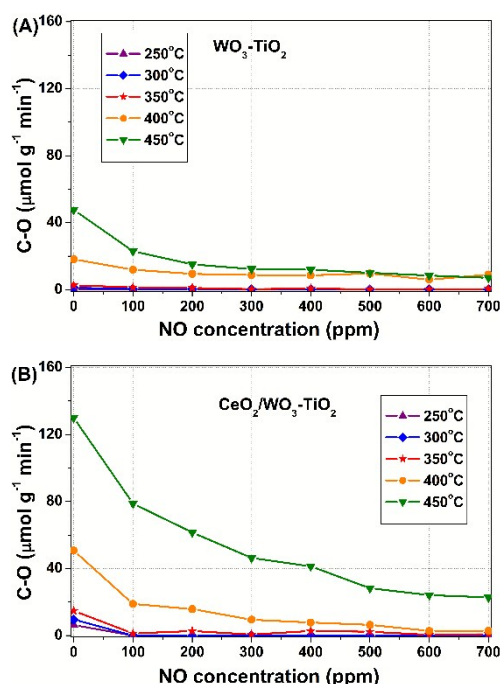


Fig. 6 C-O reaction rates as a function of gaseous NO concentration over (A) WO<sub>3</sub>-TiO<sub>2</sub> and (B) CeO<sub>2</sub>/WO<sub>3</sub>-TiO<sub>2</sub>. Reaction conditions: [NO] = 0-700 ppm, [NH<sub>3</sub>] = 500 ppm, [O<sub>2</sub>] = 5 vol.%, N<sub>2</sub> balance and catalyst mass = 3-200 mg.

**3.5.3 NSCR reaction rates** The NSCR reaction (represented by N<sub>2</sub>O formation) rates as a function of NO concentration over WO<sub>3</sub>-TiO<sub>2</sub> and CeO<sub>2</sub>/WO<sub>3</sub>-TiO<sub>2</sub> were shown in Fig. 7. The NSCR reaction rates of CeO<sub>2</sub>/WO<sub>3</sub>-TiO<sub>2</sub> were much lower than those of WO<sub>3</sub>-TiO<sub>2</sub>, which is consistent with the low N<sub>2</sub>O formation of CeO<sub>2</sub>/WO<sub>3</sub>-TiO<sub>2</sub> during SCR activity test in Fig. 1(B).

With the increase of NO concentration, the NSCR reaction rates over WO<sub>3</sub>-TiO<sub>2</sub> increased gradually, and the reaction rates remarkably correlated with NO concentration, with the liner correlation coefficients all above 0.957, indicating that the reaction order of NSCR with respect to NO concentration over WO<sub>3</sub>-TiO<sub>2</sub> was 1. This result is different with the previously reported reaction order of 0 over MnO<sub>x</sub>-based catalysts.<sup>20,24</sup> In addition, the reaction order over CeO<sub>2</sub>/WO<sub>3</sub>-TiO<sub>2</sub> was nearly 0, especially at high temperature region.

The NSCR reaction mainly follows the Eley-Rideal mechanism, i.e., adsorbed NH<sub>3</sub> species react with gaseous NO to form N<sub>2</sub>O, as demonstrated by the transient reaction study in Fig. 3. Due

to the low SCR and C-O reaction rates, the consumption of adsorbed NH<sub>3</sub> species over WO<sub>3</sub>-TiO<sub>2</sub> was relatively low, thus the adsorbed NH<sub>3</sub> species on the surface of WO<sub>3</sub>-TiO<sub>2</sub> would probably be sufficient for the NSCR reaction. Therefore, the reaction order of NSCR with respect to NO concentration could be 1.

Usually, the N<sub>2</sub>O formation increase gradually with the reaction temperature during SCR reaction. Interestingly, we found that N<sub>2</sub>O formation over WO<sub>3</sub>-TiO<sub>2</sub> exhibited a decrease trend over 350 °C in the SCR performance tests, as shown in Fig. 1(B). However, the N<sub>2</sub>O formation kept increase during NH<sub>3</sub> oxidation test in the absence of NO. To investigate the reason for the decrease of N<sub>2</sub>O formation over WO<sub>3</sub>-TiO<sub>2</sub>, the N<sub>2</sub>O selectivity during SCR activity test and the kinetic test were both calculated by the following equation:

$$\text{N}_2\text{O selectivity} = \frac{2[\text{N}_2\text{O}]_{\text{out}}}{[\text{NO}_x]_{\text{in}} + [\text{NH}_3]_{\text{in}} - [\text{NO}_x]_{\text{out}} - [\text{NH}_3]_{\text{out}}} \times 100\%$$

$$= 1 - \text{N}_2 \text{ selectivity} \quad (14)$$

Similar with that of N<sub>2</sub>O formation, both of the N<sub>2</sub>O selectivity during activity test and kinetic test decreased gradually from 350 to 450 °C (Fig. 8). Considering the relatively high SCR reaction rates at 400 and 450 °C (Fig. 5A), the decrease of N<sub>2</sub>O selectivity indicates intense competition between SCR and NSCR reactions at high temperatures over WO<sub>3</sub>-TiO<sub>2</sub>, which should be the main reason for the decrease of N<sub>2</sub>O formation.

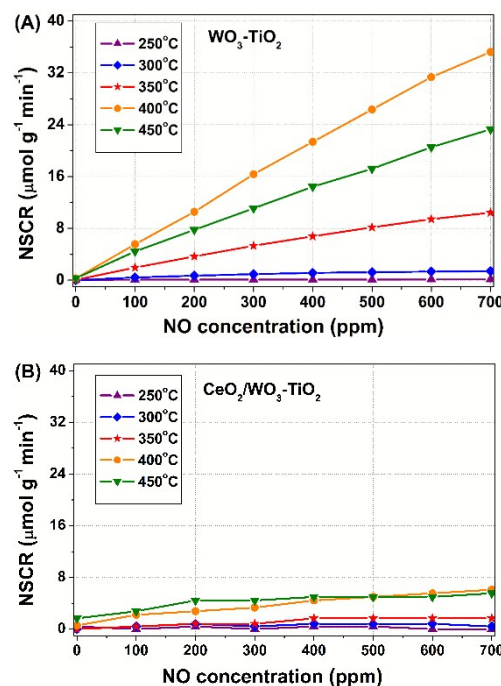


Fig. 7 NSCR reaction rates as a function of gaseous NO concentration over (A) WO<sub>3</sub>-TiO<sub>2</sub> and (B) CeO<sub>2</sub>/WO<sub>3</sub>-TiO<sub>2</sub>. Reaction conditions: [NO] = 0-700 ppm, [NH<sub>3</sub>] = 500 ppm, [O<sub>2</sub>] = 5 vol.%, N<sub>2</sub> balance and catalyst mass = 3-200 mg.

With the introduction of CeO<sub>2</sub>, the CeO<sub>2</sub>/WO<sub>3</sub>-TiO<sub>2</sub> showed remarkably enhanced SCR reaction rate, and thus depressed the NSCR reaction. Therefore, the N<sub>2</sub>O formation over CeO<sub>2</sub>/WO<sub>3</sub>-TiO<sub>2</sub> was very low. Without the feed of gaseous NO, SCR

reaction was inhibited during  $\text{NH}_3$  oxidation test. Therefore, both of the  $\text{N}_2\text{O}$  formations over  $\text{WO}_3\text{-TiO}_2$  and  $\text{CeO}_2/\text{WO}_3\text{-TiO}_2$  increased gradually with the reaction temperature.

Previous studies on the mechanism of  $\text{N}_2\text{O}$  formation in  $\text{NH}_3$  oxidation have revealed a two-step reaction pathway involving  $\text{NO}$  as an intermediate: (1)  $\text{NH}_3$  is first oxidized to  $\text{NO}$  by  $\text{O}_2$  (C-O reaction), and then (2) the  $\text{NO}$  react with adsorbed  $\text{NH}_3$  species to form  $\text{N}_2\text{O}$  (NSCR reaction).<sup>32,35-37</sup> Therefore, the higher C-O reaction rate over  $\text{CeO}_2/\text{WO}_3\text{-TiO}_2$  resulted in higher  $\text{NO}$  formation and thereby induced higher  $\text{N}_2\text{O}$  formation during the  $\text{NH}_3$  oxidation in this study (Fig. 2B).

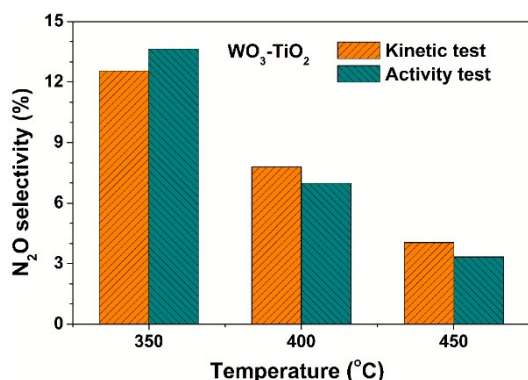


Fig. 8  $\text{N}_2\text{O}$  selectivity in the  $\text{NH}_3\text{-SCR}$  reactions over  $\text{WO}_3\text{-TiO}_2$  during kinetic study and activity test. Reaction conditions:  $[\text{NO}] = [\text{NH}_3] = 500$  ppm,  $[\text{O}_2] = 5$  vol.%, and  $\text{N}_2$  balance.

## Conclusions

The effects of  $\text{CeO}_2$  for a high-efficiency  $\text{CeO}_2/\text{WO}_3\text{-TiO}_2$  catalyst on the  $\text{N}_2\text{O}$  formation during  $\text{NH}_3\text{-SCR}$  reaction were investigated by kinetic method. Interestingly, we found that  $\text{CeO}_2$  was effective for the inhibition of  $\text{N}_2\text{O}$  formation under SCR reaction condition over the catalyst, while it enhanced the  $\text{N}_2\text{O}$  formation under  $\text{NH}_3$  oxidation reaction condition. The kinetic investigations showed that  $\text{CeO}_2$  is very effective for enhancing SCR and C-O reaction rates and depressing the NSCR reaction. Therefore, the  $\text{N}_2\text{O}$  formation under SCR reaction condition could be remarkably inhibited due to the competition between SCR and NSCR reactions. On the other hand, under  $\text{NH}_3$  oxidation condition without the feed of gaseous  $\text{NO}$ , the enhanced C-O reaction promoted  $\text{N}_2\text{O}$  formation due to the lack of SCR reaction.

In addition, we found another interesting phenomenon that the  $\text{N}_2\text{O}$  formation over  $\text{WO}_3\text{-TiO}_2$  decreased gradually at high temperature from 350 to 450 °C, but when  $\text{CeO}_2$  was introduced the  $\text{N}_2\text{O}$  formation kept increasing with the reaction temperature over  $\text{CeO}_2/\text{WO}_3\text{-TiO}_2$ . The different  $\text{N}_2\text{O}$  formation profiles of the two catalysts was also associated with the promotional effect of  $\text{CeO}_2$  on SCR reaction and the competition between SCR and NSCR reactions.

## Acknowledgements

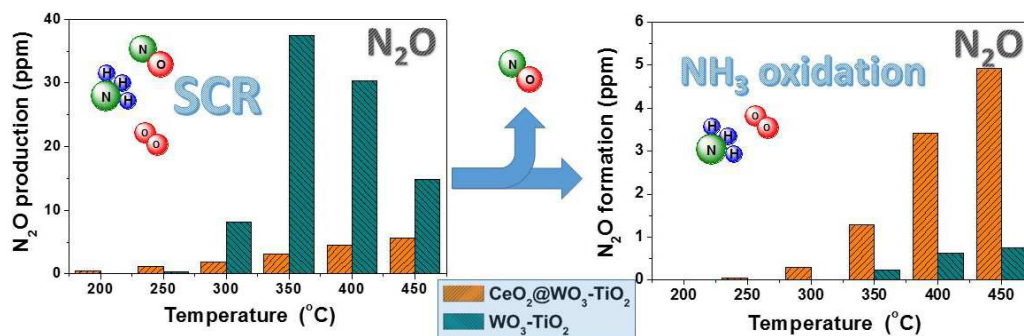
The authors gratefully acknowledge the financial supports from the National Natural Science Foundation of China (51308296), the Qing Lan Project of Jiangsu Province, China, and the Fundamental Research Funds for the Central Universities (30920140111012).

## References

- G. Busca, L. Lietti, G. Ramis and F. Berti, *Appl. Catal., B*, 1998, **18**, 1-36.
- B. Guan, R. Zhan, H. Lin and Z. Huang, *Appl. Therm. Eng.*, 2014, **66**, 395-414.
- M. Koebel, M. Elsener and M. Kleemann, *Catal. Today*, 2000, **59**, 335-345.
- P. Granger and V. I. Parvulescu, *Chem. Rev.*, 2011, **111**, 3155-3207.
- S. Brandenberger, O. Kröcher, A. Tissler and R. Althoff, *Catal. Rev.*, 2008, **50**, 492-531.
- U. Deka, I. Lezcano-Gonzalez, B. M. Weckhuysen and A. M. Beale, *ACS Catal.*, 2013, **3**, 413-427.
- Z. Liu, J. Zhu, J. Li, L. Ma and S. I. Woo, *ACS Appl. Mater. Interfaces*, 2014, **6**, 14500-14508.
- Z. Wu, R. Jin, Y. Liu and H. Wang, *Catal. Commun.*, 2008, **9**, 2217-2220.
- Z. Liu, J. Zhu, J. Li, L. Ma and S. I. Woo, *Appl. Catal., B*, 2014, **158-159**, 11-19.
- R. Q. Long and R. T. Yang, *J. Am. Chem. Soc.*, 1999, **121**, 5595-5596.
- W. Shan, F. Liu, H. He, X. Shi and C. Zhang, *Chem. Commun.*, 2011, **47**, 8046-8048.
- Y. Peng, R. Qu, X. Zhang and J. Li, *Chem. Commun.*, 2013, **49**, 6215-6217.
- Z. Liu, S. Zhang, J. Li and L. Ma, *Appl. Catal., B*, 2014, **144**, 90-95.
- Z. Liu, Y. Yi, J. Li, S. I. Woo, B. Wang, X. Cao and Z. Li, *Chem. Commun.*, 2013, **49**, 7726-7728.
- W. Shan, F. Liu, H. He, X. Shi and C. Zhang, *Appl. Catal., B*, 2012, **115-116**, 100-106.
- Z. Si, D. Weng, X. Wu, J. Yang and B. Wang, *Catal. Commun.*, 2010, **11**, 1045-1048.
- C. Liu, L. Chen, H. Chang, L. Ma, Y. Peng, H. Arandiyani and J. Li, *Catal. Commun.*, 2013, **40**, 145-148.
- W. Shan, F. Liu, Y. Yu and H. He, *Chin. J. Catal.*, 2014, **35**, 1251-1259.
- H. Huang, W. Shan, S. Yang and J. Zhang, *Catal. Sci. Technol.*, 2014, **4**, 3611-3614.
- S. Yang, S. Xiong, Y. Liao, X. Xiao, F. Qi, Y. Peng, Y. Fu, W. Shan and J. Li, *Environ. Sci. Technol.*, 2014, **48**, 10354-10362.
- P. R. Ettireddy, N. Ettireddy, T. Boningari, R. Pardemann and P. G. Smirniotis, *J. Catal.*, 2012, **292**, 53-63.
- S. Xiong, Y. Liao, X. Xiao, H. Dang and S. Yang, *Catal. Sci. Technol.* 2015, **5**, 2132-2140.
- S. Yang, Y. Fu, Y. Liao, S. Xiong, Z. Qu, N. Yan and J. Li, *Catal. Sci. Technol.*, 2014, **4**, 224-232.
- S. Yang, Y. Liao, S. Xiong, F. Qi, H. Dang, X. Xiao and J. Li, *J. Phys. Chem. C*, 2014, **118**, 21500-21508.
- L. Chen, J. Li and M. Ge, *Environ. Sci. Technol.*, 2010, **44**, 9590-9596.
- Z. Wu, B. Jiang, Y. Liu, H. Wang and R. Jin, *Environ. Sci. Technol.*, 2007, **41**, 5812-5817.
- W.S. Kijlstra, D.S. Brands, H.I. Smit, E.K. Poels and A. Bliet, *J. Catal.*, 1997, **171**, 208-218.
- F. Liu, H. He, Y. Ding and C. Zhang, *Appl. Catal. B*, 2009, **93**, 194-204.
- N.Y. Topsøe, *Science*, 1994, **265**, 1217-1219.

- 30 P.G. Smirniotis, D.A. Peña and B.S. Uphade, *Angew. Chem. Int. Ed.*, 2001, **40**, 2479-2482.
- 31 G. Qi, R.T. Yang and R. Chang, *Appl. Catal. B*, 2004, **51**, 93-106.
- 32 L. Zhang and H. He, *J. Catal.*, 2009, **268**, 18-25.
- 33 S. Yang, F. Qi, Y. Liao, S. Xiong, Y. Lan, Y. Fu, W. Shan and J. Li, *Ind. Eng. Chem. Res.*, 2014, **53**, 5810-5819.
- 34 I. Nova, D. Bounechada, R. Maestri, E. Tronconi, A. K. Heibel, T. A. Collins and T. Boger, *Ind. Eng. Chem. Res.*, 2010, **50**, 299-309.
- 35 J. Perez-Ramirez and E. V. Kondratenko, *Chem. Commun.*, 2004, 376-377.
- 36 Z. Qu, H. Wang, S. Wang, H. Cheng, Y. Qin and Z. Wang, *Appl. Surf. Sci.*, 2014, **316**, 373-379.
- 37 A. C. Akah, G. Nkeng and A. A. Garforth, *Appl. Catal., B*, 2007, **74**, 34-39.





The effect of CeO<sub>2</sub> for a high-efficiency CeO<sub>2</sub>/WO<sub>3</sub>-TiO<sub>2</sub> catalyst on the N<sub>2</sub>O formation in NH<sub>3</sub>-SCR reaction was investigated using kinetic method.